Proceedings of the 15th International Symposium on the Packaging and Transportation of Radioactive Materials
PATRAM 2007
October 21-26, 2007, Miami, Florida, USA

NUMERICAL SIMULATION OF THE ONE METER DROP TEST ON A BAR FOR THE CASTOR CASK

Nikola Jakšić **Karl-Fredrik Nilsson**
European Commission, DG-JRC, Institute for Energy,
P.O. Box 2, 1755 ZG Petten, The Netherlands

ABSTRACT

This paper presents a numerical analysis of the 1m drop test on a steel bar of a Castor AVR cask and where the impact is in a region with fins as well as in a region where the fins have been locally removed. The paper consists of two parts: i) a parameter study with an overall objective to derive an analysis methodology and ii) comparison with experimental data. The parameter study includes parameters that can not be, or were not, defined directly from the experimental data as well as parameters linked to the numerical procedures within FEM. The parameters are validated by their influence on the model responses and effort needed for the assessment of their appropriate values. Then the model with the "best" parameter set is verified against the experimental results. The agreement between experimental and simulation results are very good.

INTRODUCTION

The integrity of waste packages is crucial for the safe disposal, storage and transport of spent nuclear fuel and radioactive waste. For certification the manufacturers need to demonstrate that the waste packages can withstand loads that could occur under operation and accident conditions [1]. This can be done full-scale testing or simulation. The drop tests are very expensive. There is therefore a trend to replace testing by numerical analyses. Apart from cost saving the numerical simulations allows parameter studies and assessment of safety margins and better understanding of the system performance.

This paper describes a numerical analysis of a 1m drop test on a steel bar of a Castor AVR cask proposed by GNS [2] to evaluate different modelling aspects, Figure 1. The cask comes from the CASTOR family with machined cooling fins in a region where impact occurs. In the first test, the impact is on the cask's cooling fins (*finned drop case*) whereas in the second test the impact is in an area where the fins have been locally machined away (*flat drop case*). The problem has a direct practical implication since the effect of the cask's cooling fins on the impact behaviour is not completely understood. The objective of the numerical simulation was to assess the relevance of a number of parameters with respect to computational effort and their influence to the basic results. The numerical analysis is based on a so called explicit dynamic analysis using the commercial finite element code ABAQUS extended with Python scripts to allow a parametric description of the problem.

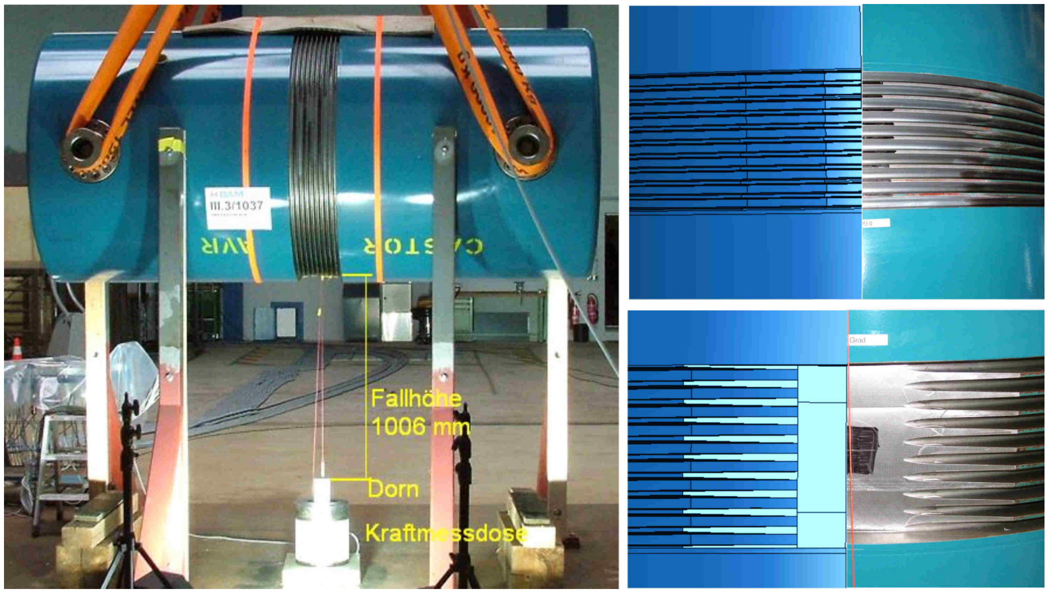

a) b)

Figure 1. a) The experimental set up b) the model and photograph of impact region for "finned drop case" and "flat drop case"

MODEL DESCRIPTION

The finite element model consists of the cask's body, the lid, the bar and the rigid surface representing the upper surface of the force transducer on which the bar is fixed with a screw, Figure 2. The free fall is modelled by prescribing the initial velocity of the cask positioned directly above the bar. The only load defined in the model is gravity. Symmetry is assumed and hence, only one half of the set up is modelled, Figure 2a. A rigid fixed surface is modelled below the bar in order to model the frictional contact between the bar and the force transducer. The portion of the bottom surface where the bar is attached to the force transducer by a screw is clamped. The remaining part of the bar's bottom has been modelled as clamped, free sliding as well as with general contact algorithm using penalty method. The contact between the bar and the rigid surface is then modelled as surface-to-surface contact applying the kinematic contact method.

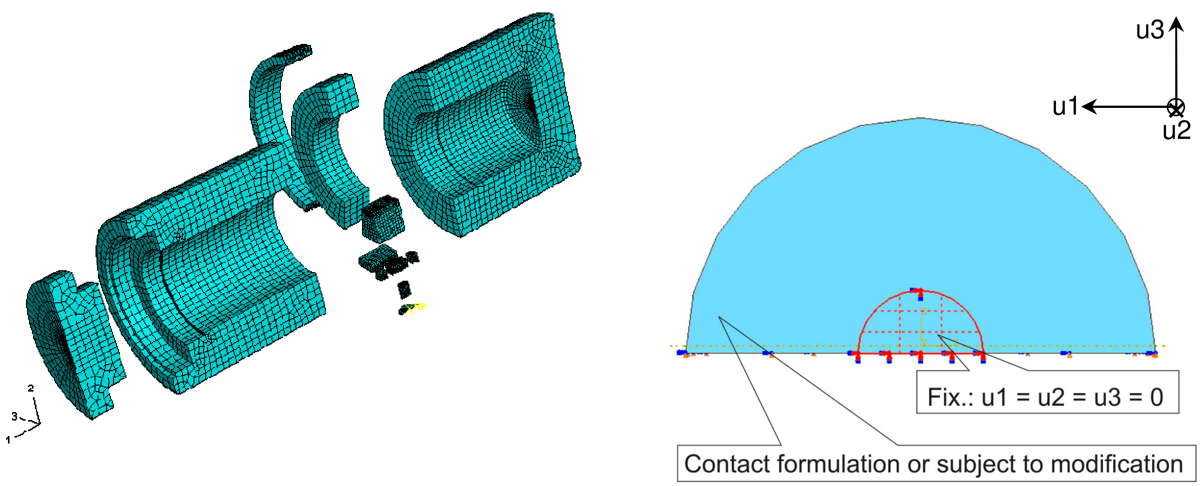

a) b)

Figure 2. a) Mesh of the expanded model showing the symmetry plane and b) boundary conditions at the bar's bottom surface.

PARAMETER STUDY

Eight different parameters were studied ranked by influence on the model responses:

1) element size (*10mm*),
2) element type (*hex*),
3) material model (*tabular*),
4) mass scaling (*none*),
5) boundary conditions (*contact*),
6) coefficient of friction (*0.2*),
7) hourglass control (*enhanced*),
8) bulk viscosity (*0.03, 0.6*).

The appropriate values of the parameters from (1) to (7) were determined by comparing computed and experimental results whereas for (8) the minimum of the artificial energy was the measure for the value determination. The "Base Model" parameter values are given in brackets. Only (1), (3), (5) and (6) are presented in more detail in this paper, Figure 3. In this figure the parameters are organized according to the impact on the model response and effort needed either for the estimation of their values or for computational time. Some influences on the model response of the parameters not specifically presented in this paper are summarized in the conclusions. Element type (2) analysis showed that the preferred element type is hexagonal. Mass scaling (4) should be used with at most care and should not in any case exceed 8. There is no single optimal hourglass control (7) for all cases. However, the enhanced hourglass control works relatively well. Default values of the bulk viscosity should be decreased in order to decrease the artificial energy. Parameters' values for the Base Model were established on the basis on the measurements, the engineering common sense and solver predefined values. Only the results of the flat drop case are presented in parameter study as the finned drop case results essentially communicate the same message.

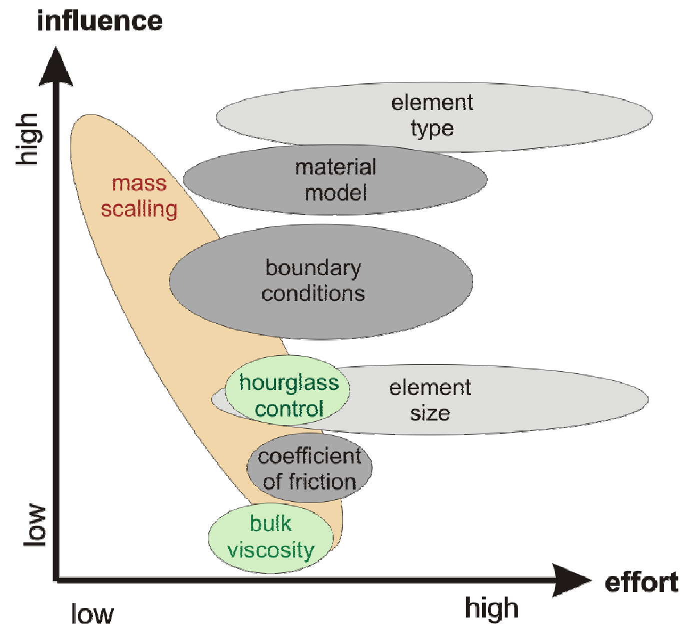

Figure 3. Qualitative presentation of the parameters according to their *influence* on model responses and either computational *effort* or *effort* to estimate the parameter's value

Element size

Element sizes were varied predominantly in the vicinity of the impact area, Figure 4. The element sizes in Table 1 are the required values for mesher in the impact region; actual element sizes may vary by a small amount. As seen in Table 1, the computational effort increases exponentially with the denser mesh. The reaction force at the bar's bottom and the maximum

Table 1. Mesh name, element size, No. of the DOF and CPU time for the flat drop case

Mesh name	Element size [mm]	DOF	CPU time [DD-HH:MM]
Coarser	15	63 159	00-04:07
Base	10	64 830	00-04:44
Finer	5	88 869	00-12:45
The finest	2	348 165	12-13:47

principal strain the cask's wall directly above the impact zone (point D1), Figure 4, are relatively insensitive to the mesh density; the scatter is less than ±5% off from Base Model, Figure 5. No monotonous convergence of results was found when analyzing different displacements, Figure 6. For other computed properties, for instance deformed shape of the bar for the finned case, there is of course significant mesh dependence.

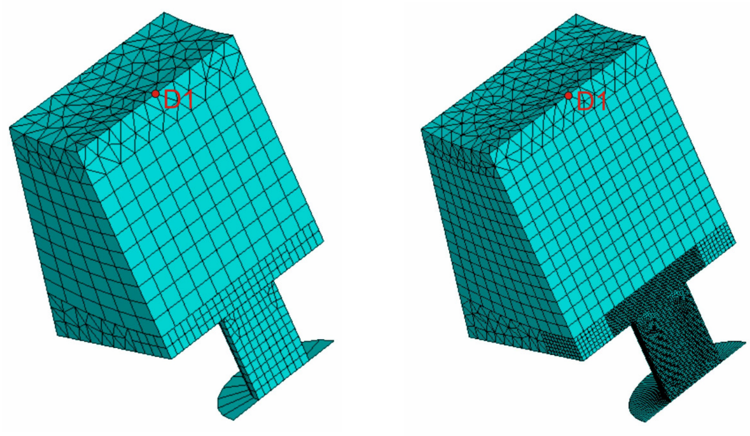

Figure 4. Base mesh (left) and the finest mesh (right)

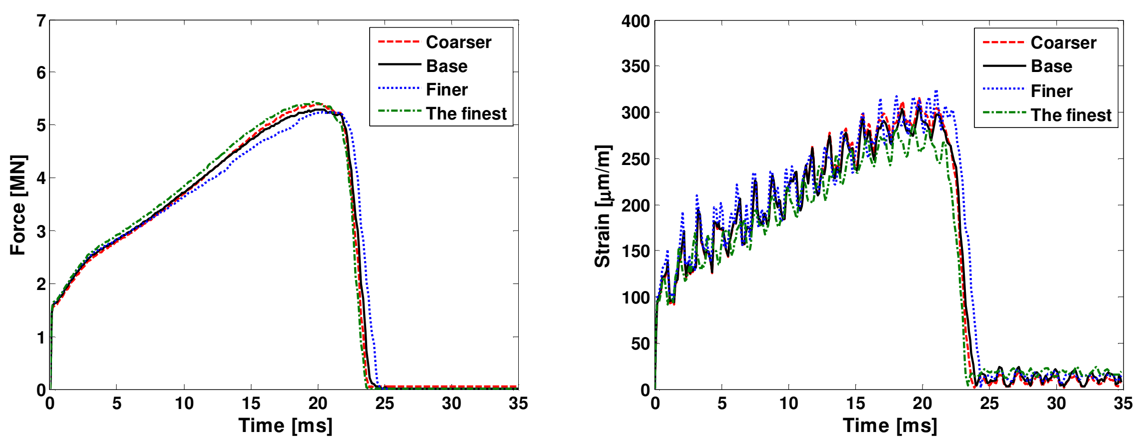

a) **b)**

Figure 5. Computed data for the flat drop case for different mesh refinements a) Reaction force b) maximal principal strain

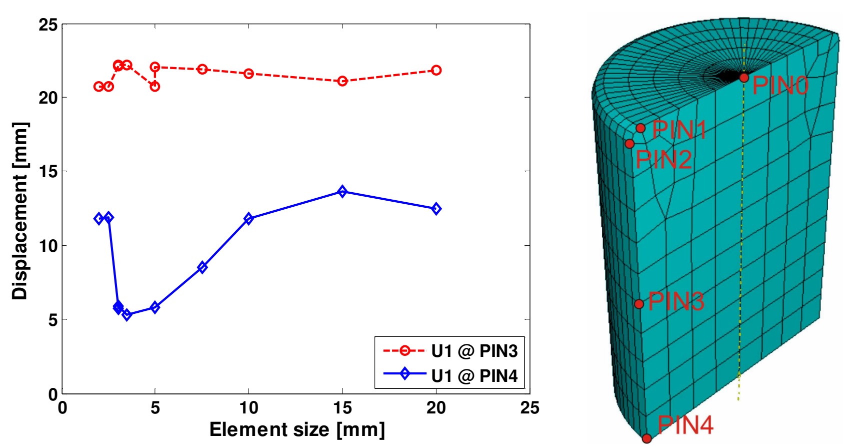

a) **b)**

Figure 6. a) Computed Horizontal displacement at PIN4 as function of mesh density for flat drop case and b) measurement points on the bar

Material model

Two different material models were compared: experimental tabular data from the tensile test and Johnson-Cook (JC) material model [5] fitted to the experimental tensile data, Figure 7. The JC model deviates from measured data for low strains with high strain rates and for high strains with small strain rates. The computed reaction force and maximum principal strain are shown in Figure 8. It can be directly concluded that the JC material model is not appropriate.

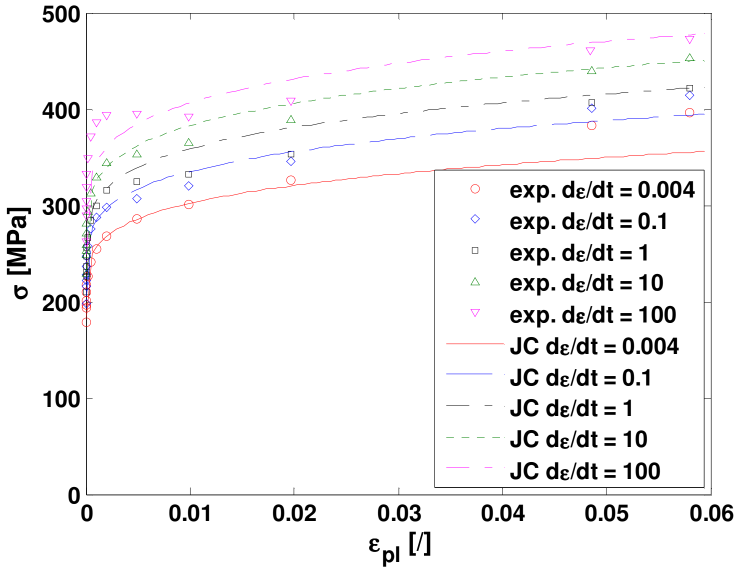

Figure 7. Measured tensile stress-strain curve and Johnson-Cook approximation

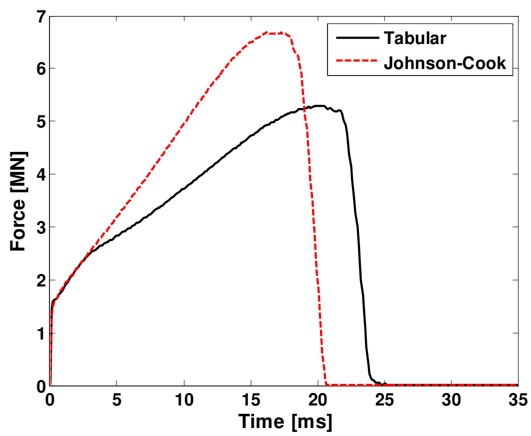

a)

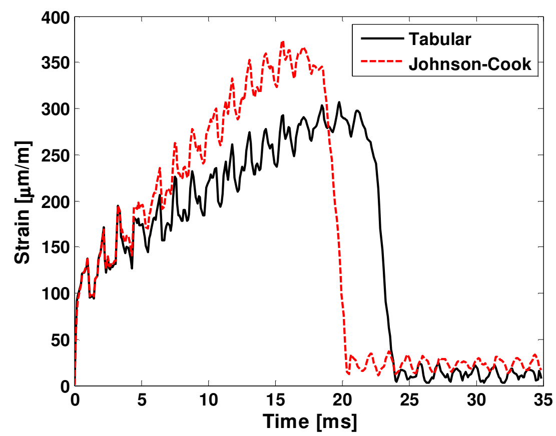

b)

Figure 8. Computed data for the flat drop case for the two material models a) Reaction force b) maximal principal strain

Boundary conditions for bar-support and coefficient of friction

Three different boundary conditions of the bar's bottom part shown in Figure 2b were investigated. For the Base Model a complete contact model was employed. For the second case, “bc-1”, the bar can slide freely (i.e. no friction contact) and zero vertical displacement is imposed. For the third case, “bc-2”, the area is clamped (zero vertical and horizontal displacements imposed). The computed reaction force and maximum principal strain for the three cases are plotted in Figure 9. It surprising that the results for Base case is not between the free sliding and clamped case, but the important observation is that the modelling has only a slight effect on the computed results. The qualitative comparison between simulation and experiment shows that the final shape of the bar is best simulated with the frictional contact formulation of the Base Model, Figure 10.

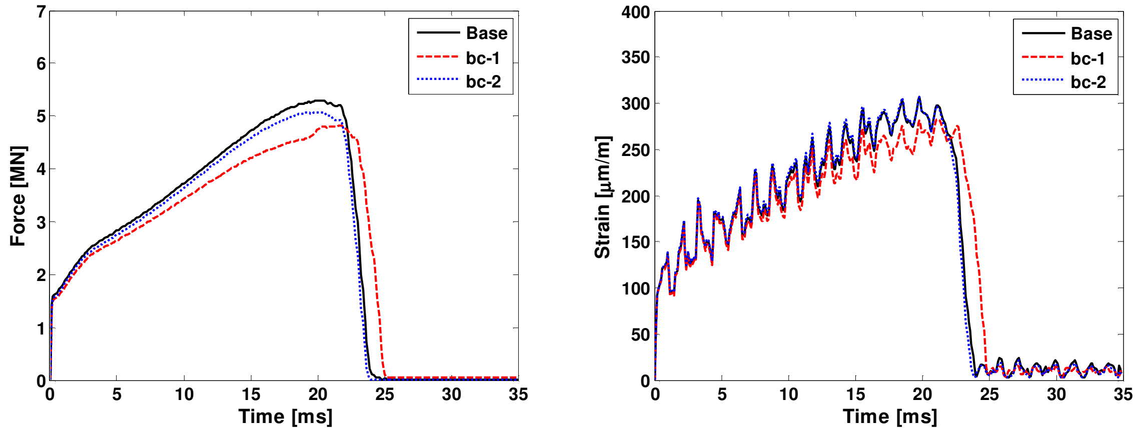

Figure 9. Computed data for the flat drop case for the three bar boundary conditions a) Reaction force b) maximal principal strain

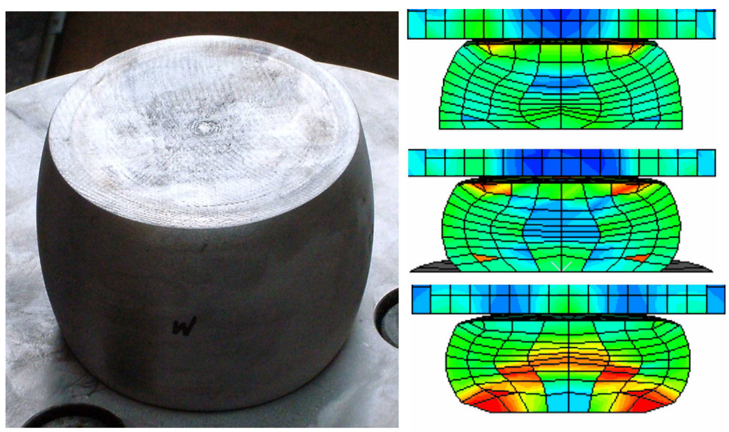

Figure 10. The bar after the flat drop (left) and simulation results (right) of the models: bc-1 (frictionless sliding), base, bc-2 clamped bottom

The variation of the coefficient of friction is not very influential on the model responses such as vertical reaction force and maximal principal strain. However, the contact friction influences the final shape of the bar, which can be used for estimation of the coefficient of friction. The horizontal displacement of the bottom edge of the bar scales linearly with the coefficient of friction, Figure 11; $y=a{\cdot}x+b$, where a=-0.038 and b=0.019 for the flat drop case and a=-0.044 and b=0.020 for the finned case.

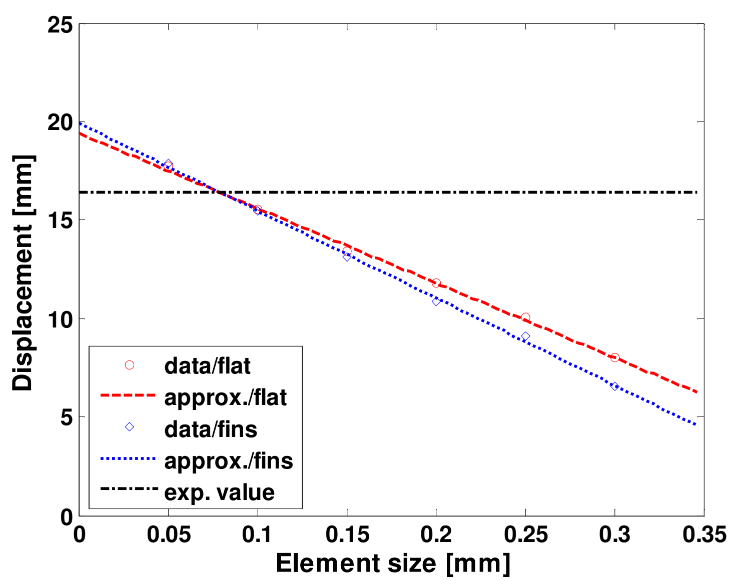

Figure 11. Linear approximation of the horizontal displacement at the bottom edge of the bar – flat drop case.

Coefficient of friction can thus be defined as 0.08. The value of the coefficient of friction between the bar and the rigid surface do not significantly influence the model responses.

MODEL VERIFICATION

The model with the "best" parameter set is compared with the experimental data: the vertical reaction force and the equivalent strain (1) at D1, Table 2 and Figure 12. The equivalent strain is defined as:

$$\varepsilon_v = \frac{1}{(1+\nu)\sqrt{2}}\sqrt{(\varepsilon_1-\varepsilon_2)^2+(\varepsilon_2-\varepsilon_3)^2+(\varepsilon_3-\varepsilon_1)^2} \tag{1}$$

Model shows that predominantly elastic strains are found at the point D1. The computed vertical reaction forces and equivalent strains are 6% lower than the measured data except for the equivalent strain for finned drop case for which the calculated value is 17% lower. The reaction force is 6% lower in the finned case than the flat in both experiment and analysis. In the experiment the equivalent strain is 19% lower for finned case in comparison to the flat drop whereas in the simulation the difference is 28%. The impact duration is consistently somewhat longer in the simulation than in the experiment but the difference between the flat and finned case are very similar

Table 2. Comparison between peak values of the reaction force, equivalent strain and horizontal bar's bottom edge displacement

Extremum of the	Unit	Drop case	Exp.	Sim.	Rel. Diff. Exp./Sim.	Rel. Diff. Flat/Fins
Reaction Force	[MN]	flat	4.769	4.479	-6 %	Exp. -6%
		fins	4.447	4.204	-5 %	Sim. -6%
Equivalent Strain	[%]	flat	0.0386	0.0361	-6 %	Exp. -19%
		fins	0.0311	0.0259	-17 %	Sim. -28%

The difference between analysis and experiment are relatively small considering the different modelling idealizations. It was shown above that there was a significant difference in the computed reaction force and strain when the Tabulated value or the Johnson-Cook models were used. It well known that ductile cast iron has much more hardening in compression than tension. It is therefore quite likely that the difference between using a model, which is harder in compression, and the present material model would be notable. Local material failure is another potential source to difference between computed and measured values. In the analysis the fins only deform plastically whereas in the test fins in the impact region separated from the cask.

CONCLUSIONS

The overall behaviour of the model is qualitatively very similar to what was observed during the experiments. The reaction force at the bar's bottom surface and the equivalent strain at the point D1 are qualitatively similar and quantitatively somewhat lower in the simulation than in the experiment.

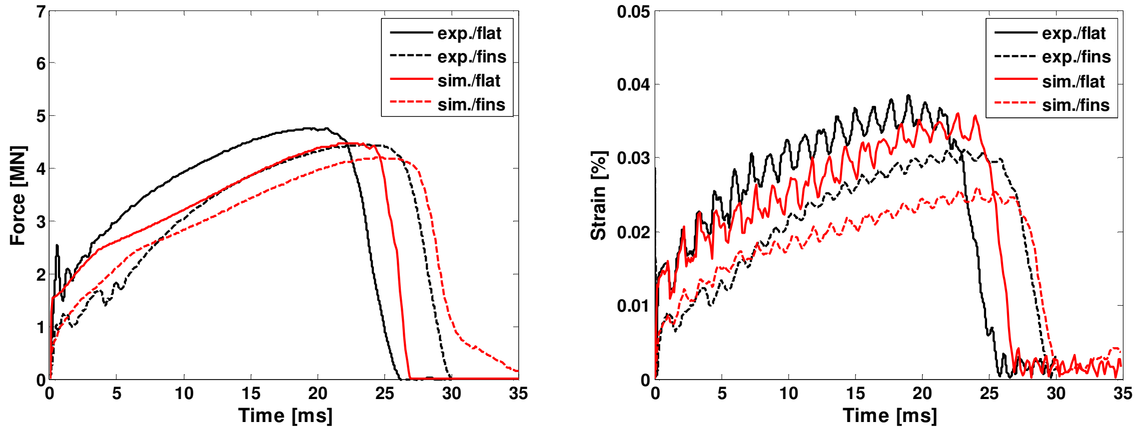

Figure 12. Comparison between experiment and simulation; reaction force (left) and equivalent strain (right)

The sensitivity analysis was performed to study the influence of different parameters that either were not defined directly from the experimental data or that are linked to the FE numerical procedures. **(i)** The Johnson-Cook model is not adequate for the material under consideration. **(ii)** Tetrahedral elements should be avoided if possible, see [3]. **(iii)** No monotonous convergence of the responses was found when increasing the mesh density of the model. **(iv)** Supporting boundary conditions with the implemented contact seems to produce best results. **(v)** Mass scaling should be used with caution and the mass scaling factor should not exceed value of 8, see [4]. **(vi)** Variation of the coefficient of friction between the bar and the rigid surface scatters the model responses to up to ±5% around "Base Model" results. The value of the coefficient of friction is estimated on 0.08.

ACKNOWLEDGMENTS

This work has been founded under the European Commission and it is part of the JRC Action: SAFEWASTE. The authors are also pleased to acknowledge GNS (Gesellschaft für Nuklear-Service mbH) from Germany for their interest and support.

REFERENCES

[1] IAEA Safety Standards Series, Advisory Material for the IAEA Regulations for the Safe Transport of Radioactive Material, Safety Guide, No. TS-G-1.1 (ST-2), International Atomic Energy Agency, Vienna, June 2002

[2] R. Hueggenberg, H.-P. Winkler, J.Holtorf, (2007), Comparison of the behavior of a finned and unfinned surface during a drop test of a cask onto a steel bar, *PATRAM 2007, Miami, Florida USA, October 21-26, 2007*

[3] N. Jakšić, K.-F. Nilsson, (2007), *Numerical simulation of the one meter drop test on a bar for the Castor cask - Initial and sensitivity analysis*, European Commission, DG JRC, Insistute for Energy, Petten, EUR22470EN; http://www.jrc.nl/publications/scientific_publications/2007/EUR22470EN.pdf

[4] N. Jakšić, K.-F. Nilsson, (2007), *Numerical simulation of the one meter drop test on a bar for the Castor cask – Advanced and final analyses*, European Commission, DG JRC, Insistute for Energy, Petten

[5] G.R. Johnson and W.H. Cook, (1985). Fracture characteristics of three metals subjected to various strains, strain rates, temperatures and pressures. *Engineering Fracture Mechanics*, **21**(1), 31-48.